Parametric mechanism maintaining Couette flow turbulence is verified in DNS

By B. F. Farrell†, P. J. Ioannou‡ AND M.-A. Nikolaidis‡

The no-slip boundary condition results in a velocity shear forming in fluid flow near a solid surface. This shear flow supports the turbulence characteristic of fluid flow near boundaries at Reynolds numbers above ≈ 1000 by making available to perturbations the kinetic energy of the externally forced flow. Understanding the physical mechanism underlying transfer of energy from the forced mean flow to the turbulent perturbation field that is required to maintain turbulence poses a fundamental question. Although qualitative understanding that this transfer involves nonlinear destabilization of the roll-streak coherent structure has been established, identification of this instability has resisted analysis. This instability has resisted comprehensive analysis because its analytic expression lies in the Navier–Stokes equations (NS) expressed with statistical rather than state variables. Expressing NS as a statistical state dynamics (SSD) at second order in a cumulant expansion suffices to allow analytical identification of the nonlinear roll-streak instability underlying turbulence in wall-bounded shear flow. In this nonlinear instability the turbulent perturbation field is identified by the SSD, with the Lyapunov vectors (LVs) of the linear operator governing perturbation evolution about the time-dependent streamwise mean flow. In this work the implications of the predictions of SSD analysis that this parametric instability underlies the dynamics of turbulence in Couette flow and that the perturbation structures are the associated LVs, are shown to imply new conceptual approaches to controlling turbulence. It is shown that the perturbation component of turbulence is supported by the parametric instability of the streamwise mean flow, which implies optimal control should be formulated to suppress perturbations from the streamwise mean. It is also shown that suppressing only the top few LVs on the streamwise mean vectors results in laminarization. These results are verified by DNS.

1. Introduction

Analogy with the conventional interpretation of the dynamics of isotropic homogeneous turbulence forced at large scale suggests that in the turbulence of wall-bounded shear flows nonlinearity leads to a cascade of energy from the large scales, where energy is input by pressure gradients or boundary motions, to the small scales, where it is dissipated, and that the turbulence field should be essentially structureless. However, experimental studies (Kline *et al.* 1967; Bakewell & Lumley 1967; Kim *et al.* 1971; Blackwelder & Eckelmann 1979; Robinson 1991; Adrian 2007) and analysis of direct numerical simulations (DNS) (Kim *et al.* 1987; Jiménez & Moin 1991) have revealed distinct coherent structures in wall-turbulence that are believed to be essential to the process maintaining the turbulence by some form of nonlinear regeneration cycle (Kim *et al.* 1971; Jiménez 1994; Hamilton *et al.* 1995). This cycle involves a specific coherent structure rather than

† Department of Earth and Planetary Sciences, Harvard University
‡ Department of Physics, National and Kapodistrian University of Athens, Greece

unstructured fluctuations and is referred to as the self-sustaining process (SSP) (Hamilton *et al.* 1995; Waleffe 1997; Jiménez & Pinelli 1999). These coherent structures are streaks, that is, localized regions of increased or decreased velocity in the streamwise direction, and quasi-cylindrical vortices with axes oriented in the streamwise direction, called rolls, which are collocated with the low- and high-speed streaks. The SSP is associated with spatially and temporally fluctuating low-speed streaks produced by the lift-up of low-speed fluid by the rolls.† Mechanistic explanations for this process posit either that a component of the perturbations from the streamwise mean flow directly comprises the roll that forces the streak (Jiménez & Pinelli 1999; Schoppa & Hussain 2000, 2002; Adrian 2007) or that the roll is forced by perturbation Reynolds stresses that induce torques collocated correctly to maintain the rolls that in turn force the streaks through the lift-up process (Hamilton *et al.* 1995). A number of physical mechanisms have been invoked to explain the origin of the perturbations and their mechanism of action in producing this cycle. In one view the perturbations are the unstable modes of the streak (Waleffe 1997); in another they are ascribed to growth of highly amplifying transient perturbations in the flow (Schoppa & Hussain 2002). However, simply invoking such mechanisms by itself only allows qualitative descriptions to be made for hypothesized processes rather than constituting an analytical formulation that would provide a theory based directly on the equations of motion, with the property of making specific testable predictions for observational correlates.

Another approach involves exact nonlinear solutions of the Navier–Stokes equations (NS) (Waleffe 1998, 2001; Kawahara & Kida 2001). These solutions have been found at low Reynolds numbers and shown to be at times approached by turbulent state trajectories (cf. Budanur *et al.* 2017). They provide heuristic examples of the SSP process, but these solutions are not themselves fully turbulent states and they are not physically realizable as they are unstable and their physical significance to fully developed turbulence has not been established.

The SSP was recently isolated directly from the equations of motion by showing it to be inherent to and contained in a highly simplified second-order closure of the NS for wall-turbulence (Farrell & Ioannou 2012; Farrell *et al.* 2017). This SSD isolates the nonlinear instability that underlies the SSP, and the turbulence that develops under this second-order closure has been demonstrated to be realistic and to capture the large-scale dynamics of Navier–Stokes turbulence (Thomas *et al.* 2014, 2015; Bretheim *et al.* 2015; Farrell *et al.* 2016, 2017; Pausch *et al.* 2018). This closure constitutes a quasi-linear dynamics that greatly simplifies analysis while having the attribute of not only allowing identification of the dynamics supporting the large-scale roll-streak coherent structures but also analytically characterizing the perturbation structures responsible for maintaining the cycle. This closure constitutes a theory for wall-turbulence in the sense that it is derived from the NS, allows identification of and analytical solution for the dynamical mechanism underlying the turbulence, and makes verifiable predictions for the structure of both the mean flow and perturbations as well as their specific roles in turbulence dynamics.

†For the purpose of formulating the SSD used in this work, we partition the flow into its streamwise mean component and perturbations. In this streamwise mean partition the roll-streak structure is included in the mean flow. From the point of view of a partition into time or ensemble means the roll-streak would be included with the perturbation field. However, the latter partitions do not result in expression in their associated SSD of the fundamental dynamics of wall-turbulence.

$[L_x, L_z]/h$	$N_x \times N_z \times N_y$	Re_τ	$[L_x^+, L_z^+]$
$[1.75\pi\ ,\ 1.2\pi]$	$33 \times 33 \times 35$	48.8	$[268, 184]$

TABLE 1. $[L_x, L_z]/h$ is the domain size in the streamwise and spanwise directions. N_x, N_z are the number of Fourier components after dealiasing with the 1/3 rule and N_y is the number of equally spaced points in the wall-normal direction. $Re_\tau = u_\tau h/\nu$ is the Reynolds number based on the friction velocity $u_\tau = \nu\, du/dy|_{y=h}$, and $[L_x^+, L_z^+]$ is the channel size in wall units ν/u_τ.

In this report we verify the perturbation structure predictions of this second-order closure using DNS and show that these analytically characterized perturbations are responsible for maintaining the turbulent state and that their removal leads to laminarization. One remarkable aspect of this identification of the perturbation structure in Navier–Stokes turbulence is that it is contrary to the common assumption that the bulk of the perturbation variance arises from an energy cascade. Instead, we show that the perturbation structures can be identified with the analytically fully characterized Lyapunov vectors (LVs) sustained by the parametric growth process associated with the fluctuating mean flow.

The remainder of this report is structured as follows. In Section 2, the formulation and computational setup are briefly outlined. Section 3 presents the main results of this study. Finally, conclusions are drawn in Section 4.

2. Formulation and computational setup

We illustrate these results using DNS for the case of Couette flow turbulence at Reynolds number $Re = 600$ ($Re = U_w h/\nu$, where $\pm U_w$ is the velocity at the channel walls at $y = \pm h$ and ν is the coefficient of kinematic viscosity). The laminar Couette flow is in the x-direction (the streamwise direction) and is given by $\mathbf{u} = (U_w y/h, 0, 0)$; y, the second component, is the cross-stream direction; and z, the third component, is the spanwise direction. The details of the DNS are given in Table 1.

We formulate the second-order SSD equations by decomposing the flow field into its streamwise mean component, denoted by $\langle\cdot\rangle_x$ or alternatively by capital letters, and the deviations from the streamwise mean, referred to as perturbation components and denoted with a dash, or equivalently into the $k_x = 0$ and the $k_x \neq 0$ components of the Fourier decomposition of the flow field, where k_x is the streamwise wave number

$$\mathbf{u} = \mathbf{U}(y,z,t) + \mathbf{u}'(x,y,z,t)\ , \quad \mathbf{U}(y,z,t) \stackrel{\text{def}}{=} \langle \mathbf{u} \rangle_x\ . \tag{2.1}$$

The NS for incompressible flow expressed using this mean and perturbation partition are

$$\partial_t \mathbf{U} + \mathbf{U}\cdot\boldsymbol{\nabla}\mathbf{U} + \boldsymbol{\nabla}P/\rho - \nu\Delta\mathbf{U} = -\langle \mathbf{u}'\cdot\boldsymbol{\nabla}\mathbf{u}'\rangle_x\ , \tag{2.2a}$$

$$\partial_t \mathbf{u}' + \mathbf{U}\cdot\boldsymbol{\nabla}\mathbf{u}' + \mathbf{u}'\cdot\boldsymbol{\nabla}\mathbf{U} + \boldsymbol{\nabla}p'/\rho - \nu\Delta\mathbf{u}' = \underbrace{-\mathbf{u}'\cdot\boldsymbol{\nabla}\mathbf{u}' + \langle \mathbf{u}'\cdot\boldsymbol{\nabla}\mathbf{u}'\rangle_x}_{N}\ , \tag{2.2b}$$

$$\boldsymbol{\nabla}\cdot\mathbf{U} = 0\ , \quad \boldsymbol{\nabla}\cdot\mathbf{u}' = 0\ , \tag{2.2c}$$

where P is the pressure and ρ the constant density. We study a turbulent Couette flow confined in a channel doubly periodic in x and z satisfying no-slip boundary conditions in the cross-stream direction: $\mathbf{U}(\pm h, z, t) = (\pm U_w, 0, 0)$, $\mathbf{u}'(x, \pm h, z, t) = (0, 0, 0)$. The mean velocity has three components $\mathbf{U}(y, z, t) = (U, V, W)$, with the cross-stream velocity V and spanwise velocity W expressible by a stream function as $V = -\partial_z \Psi$, $W = \partial_y \Psi$.

The SSD we use is closed at second order by simply setting the third cumulant to zero, which is equivalent to ignoring the perturbation-perturbation nonlinearity, N, in Eq. (2.2*b*) when formulating the SSD (Herring 1963; Farrell & Ioannou 2003). If the same term is ignored in the partition of the NS into mean and perturbations, this produces what is referred to as the restricted nonlinear (RNL) system (Thomas *et al.* 2014; Farrell *et al.* 2017)

$$\partial_t \mathbf{U} + \mathbf{U} \cdot \boldsymbol{\nabla} \mathbf{U} + \boldsymbol{\nabla} P/\rho - \nu \Delta \mathbf{U} = -\langle \mathbf{u}' \cdot \boldsymbol{\nabla} \mathbf{u}' \rangle_x \ , \tag{2.3a}$$

$$\partial_t \mathbf{u}' + \mathbf{U} \cdot \boldsymbol{\nabla} \mathbf{u}' + \mathbf{u}' \cdot \boldsymbol{\nabla} \mathbf{U} + \boldsymbol{\nabla} p'/\rho - \nu \Delta \mathbf{u}' = 0 \ , \tag{2.3b}$$

$$\boldsymbol{\nabla} \cdot \mathbf{U} = 0 \ , \quad \boldsymbol{\nabla} \cdot \mathbf{u}' = 0 \ . \tag{2.3c}$$

This RNL system has the same quasi-linear structure as the second-order SSD and can be regarded as an approximation to the second-order SSD, in which one ensemble member is used to obtain the second cumulant, and it has a number of interesting properties (Farrell & Ioannou 2017). One of these is that this system supports realistic turbulence despite the absence of nonlinearity N, which provides a constructive proof that this explicit perturbation nonlinearity is not responsible for maintaining turbulence. A second remarkable implication is that analytical identification of the perturbation structure and dynamics follows directly from analysis of Eq. (2.3*b*). Consider a self-sustaining turbulent solution of Eq. (2.3) with mean flow $\mathbf{U}(y, z, t)$. The associated perturbation field consistently satisfies Eq. (2.3*b*) with this $\mathbf{U}(y, z, t)$, which means that the perturbations evolve according to the time-dependent linear operator Eq. (2.3*b*), or symbolically

$$\partial_t \mathbf{u}' = \mathbf{A}(\mathbf{U})\, \mathbf{u}',$$

where $\mathbf{A}$ is the time-dependent linear operator. This allows complete identification of the perturbation field with the LVs of $\mathbf{A}(\mathbf{U})$. Moreover, because the turbulence supported by Eq. (2.3*b*) is bounded and nonzero, it follows that $\mathbf{u}'$ must lie in the restricted subspace spanned by the LVs of $\mathbf{A}(\mathbf{U})$ with zero Lyapunov exponent because if the Lyapunov exponent is positive, the associated vector would become unbounded and if negative it would vanish. Integration of the RNL system (Eq. (2.3)) reveals that even at moderately high Reynolds numbers this subspace is supported by a small set of streamwise harmonics,† and consequently, RNL turbulence is supported solely by these few harmonics, which provides a constructive identification of the active subspace underlying this turbulence. For example, the RNL turbulence of Couette flow at $Re = 600$ in the present channel is supported by a single LV with the gravest non-zero streamwise wave number $k_x = 2\pi/L_x$ (Farrell & Ioannou 2017). Consistently, in a realization of RNL turbulence only this perturbation component survives. In summary, we have obtained a full analytic characterization of the perturbation field that sustains RNL turbulence: it is the subspace of the LVs of $\mathbf{A}(\mathbf{U})$ with zero Lyapunov exponent. It is important to note that each ingredient of this turbulence is characterized: the coherent structures are the streamwise mean streaks, defined as the streamwise mean velocity that obtains after removal of its spanwise average, $U_s \stackrel{\text{def}}{=} U(y, z, t) - \langle U(y, z, t) \rangle_z$; the rolls with stream function Ψ collo-

† Because $\mathbf{U}$ is independent of x, each LV is supported by a single streamwise wave number. For a discussion of the streamwise harmonic support of the LVs (Thomas *et al.* 2015; Farrell *et al.* 2016).

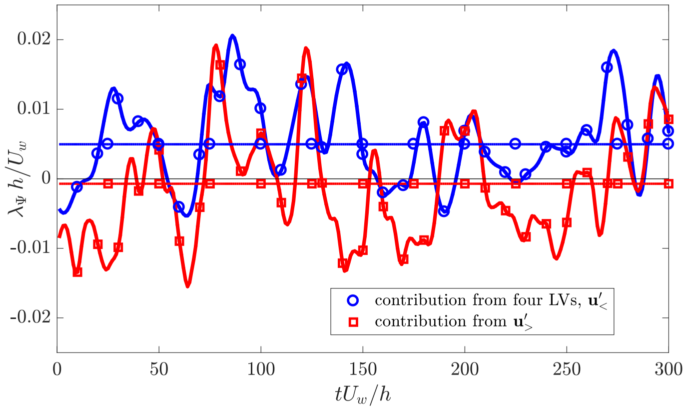

FIGURE 1. Time evolution of the contribution of the streamwise vorticity forcing, λ_Ψ, arising from the Reynolds stresses produced by $\mathbf{u}'_<$ (indicated by circles), to maintenance of the mean square stream function in the $(y-z)$ plane, Ψ^2, which largely consists of the rolls. The rate of change of the normalized streamwise square vorticity, λ_Ψ, from $\mathbf{u}'_>$ (indicated by squares) produces no net contribution to the rolls in this measure. Their time mean is indicated by the straight lines with the respective marker. This figure identifies the perturbation subspace responsible for maintaining the roll against dissipation to be the subspace spanned by the four least stable LVs.

cated with the streaks; and finally the LVs of operator $\mathbf{A}(\mathbf{U})$ with zero exponent, which are analogous to neutral modes of a time-independent linear operator. In RNL removal of the subspace of the LVs of $\mathbf{A}(\mathbf{U})$ with zero Lyapunov exponent leads immediately to laminarization.‡ We now show that removing only a few of the least stable LVs of the streamwise mean flow in a DNS suffices to laminarize the turbulence in our channel at $Re = 600$.

3. Results

The six least stable LVs of the linear operator $\mathbf{A}$ of the mean flow $\mathbf{U}(y,z,t)$ of the turbulent state in the DNS at $Re = 600$ have Lyapunov exponents

$$(0.02, 0.007, -0.0002, -0.0056, -0.013, -0.017)\, U_w/h\ .$$

The Lyapunov vectors and their exponents are calculated by evolving Eq. (2.3b) with the $\mathbf{U}(y,z,t)$ obtained from the DNS that is run in parallel. Using the standard power method and successive orthogonalizations using the energy inner-product, we obtain the LVs associated with this $\mathbf{U}(y,z,t)$ and their characteristic exponents.

As in the RNL turbulence, all of these least stable LVs are found to be supported by the gravest streamwise wave number permitted in the channel $k_x = 2\pi/L_x$† . The perturbation structure in a DNS can be projected on the basis of the orthogonalized

‡Note that these are not the more familiar LVs associated with the growth of perturbations of the trajectory of the full nonlinear system.

†Although in the RNL the Lyapunov exponents are necessarily ≤ 0 when Eq. (2.3b) is used with the $\mathbf{U}$ of the RNL, inclusion of the N term in Eq. (2.3b) results in a small component of energy loss from these vectors so that the top Lyapunov exponent consistently exceeds zero by this amount (Nikolaidis *et al.* 2018).

LVs. Doing so, we find that the perturbations in the DNS have significant projection on the first LV (11% on average) and about 20% on average on the subspace spanned by the four least stable LVs. These least stable LVs also dominate the others in the rate of energy extraction from the mean streamwise flow $U(y,z,t)$, so we anticipate that removal of these vectors should severely restrict the transfer of energy from the mean flow to the perturbations. More remarkable for our study than dominance of the energetics of the perturbations by these four least stable LVs is that they account fully for the forcing of the streamwise roll and, therefore, the SSP cycle. In order to assess the contribution of the LVs to the roll forcing, consider the equation for the streamwise component $\Omega_x = \Delta_h \Psi$ with $\Delta_h \stackrel{\text{def}}{=} \partial_y^2 + \partial_z^2$, of the mean vorticity equation

$$\partial_t \Omega_x = \underbrace{-\left(V\partial_y + W\partial_z\right)\Omega_x}_{A} + \underbrace{\nu \Delta_h \Omega_x}_{D} \underbrace{-\left[(\partial_y^2 - \partial_z^2)\langle vw\rangle_x + \partial_{yz}\left(\langle w^2\rangle_x - \langle v^2\rangle_x\right)\right]}_{G_{\Omega_x}} \ . \quad (3.1)$$

Terms A and D represent advection and dissipation of Ω_x in the $(y-z)$ plane, and if Ω_x were not acted upon by the streamwise mean vorticity forcing from the perturbation Reynolds stresses, G_{Ω_x}, the roll would decay. The contribution of perturbation Reynolds stresses to the rate of change of the normalized streamwise square vorticity, can be measured by $\lambda_{\Omega_x} = \int_V \Omega_x G_{\Omega_x} dV / (2\int_V \Omega_x^2 dV)$, and similarly, if more emphasis is to be given to the large scales, we could use as a measure the contribution of the perturbation Reynolds stresses to the maintenance of the square of the stream function. This normalized measure of this contribution to Ψ^2 is $\lambda_\Psi = \int_V \Psi G_\Psi dV / (2\int_V \Psi^2 dV)$, where $G_\Psi \stackrel{\text{def}}{=} \Delta_h^{-1} G_{\Omega_x}$ and Δ_h^{-1} is the inverse cross-stream/spanwise Laplacian. In this work we decompose the perturbation field $\mathbf{u}'$ into its component, $\mathbf{u}'_<$, projected on the subspace spanned by the four least damped energy orthonormal LVs, denoted $\mathbf{u}'_i$, $i = 1,2,3,4$ and the projection on the complement $\mathbf{u}'_>$

$$\mathbf{u}'_< \stackrel{\text{def}}{=} \sum_{i=1}^{4} (\mathbf{u}' \cdot \mathbf{u}'_i)\mathbf{u}'_i \ , \quad \mathbf{u}'_> \stackrel{\text{def}}{=} \mathbf{u}' - \mathbf{u}'_< \ , \quad (3.2)$$

and estimate G_Ψ produced by $\mathbf{u}'_<$ and $\mathbf{u}'_>$. The contribution of these subspaces to λ_Ψ is shown in Figure 1. It can be seen that the first four least stable LVs contribute 100% on average to the roll maintenance.†

This identification of a small subset of the least stable LVs as the perturbation structures that support the SSP anticipates laminarization of the turbulence in the DNS upon removal of this subspace. A long integration of the DNS of Couette turbulence at $Re = 600$ has been used to obtain the converged structures of the four least stable LVs. At a specified time the perturbation field, $\mathbf{u}'$, of the DNS is projected on the $\mathbf{u}'_<$. We remove this component of the perturbation field at an increasing rate $f(t)$ so that the perturbation field at each time step becomes $\mathbf{u}' - f(t)\delta t \mathbf{u}'_<$, where δt is the integration time step. In the example shown in Figure 2 this process of gradual removal of the first four LVs starts at $t = 100h/U_w$, so that $f(t) = 0$ for $t < 100h/U_w$ and the rate $f(t)$ increases linearly from 0 to 1 at $t = 300h/U_w$, with $f = 1$ after this time. With the gradual removal of this subspace, the entire perturbation field as well as the rolls decay leading to laminarization. The streak is seen to increase in magnitude before eventually

† The first LV contributes on average 60% to λ_Ψ, and inclusion of the second LV adds another 26%. The corresponding contribution to λ_{Ω_x} by $\mathbf{u}'_<$ is 20%, consistent with more emphasis being placed on small-scale vorticity by the square vorticity measure.

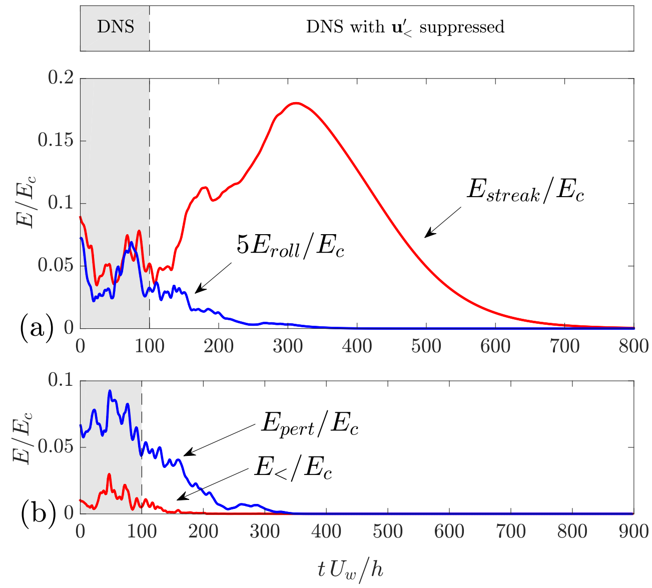

FIGURE 2. (a) Evolution of the streak energy $E_{streak} = \int_V U_s^2 dV/2$ and of the roll energy $E_{roll} = \int_V (V^2 + W^2) dV/2$ (multiplied by 5). Beginning at $t = 100h/U_w$, the component, $\mathbf{u}'_<$, that projects on the subspace spanned by the four least stable LVs is removed at an increasing rate until they are suppressed for $t > 300h/U_w$. (b) Evolution of the perturbation energy $E_{pert} = \int_V |\mathbf{u}'|^2 dV/2$ and the energy of the component that lies in the subspace of the four least stable LVs $E_< = \int_V |\mathbf{u}'_<|^2 dV/2$. All energies are normalized by the energy of the laminar Couette flow, $E_c = \int_V (U_w y)^2 dV/2h$.

decaying, as is typical of laminarization events owing to the energy extraction from the streak having been suppressed by the loss of the perturbations while the roll remains relatively more effective at continuing the lift-up process forcing the streak. In order to demonstrate that it was not the removal of perturbation energy that led to laminarization we perform the complementary experiment in which the complement $\mathbf{u}'_>$ of the four least damped LVs, accounting for 80% of the perturbation energy, is removed with the same protocol and despite that the turbulence is shown to sustain in DNS, with the perturbation structure lying in the subspace of the four least damped LVs. The corresponding evolution of the energies of the subspaces in this experiment is shown in Figure 3. The turbulence that results approaches the corresponding RNL turbulence, differing only in that the perturbation-perturbation nonlinearity introduces an additional sink for the perturbation energy. The perturbation field collapses to the single top LV of the fluctuating mean flow, as is the case for RNL turbulence in the same channel and Reynolds number (Farrell & Ioannou 2017). The turbulence that results supports rolls of approximately the same magnitude, and the streaks become stronger, as the streak is embedded in an environment of reduced eddy viscosity with the removal of the higher LVs.

4. Conclusions

In this work we have verified in a DNS of turbulent Couette flow a number of the predictions of a second-order SSD comprising the streamwise mean flow and the second

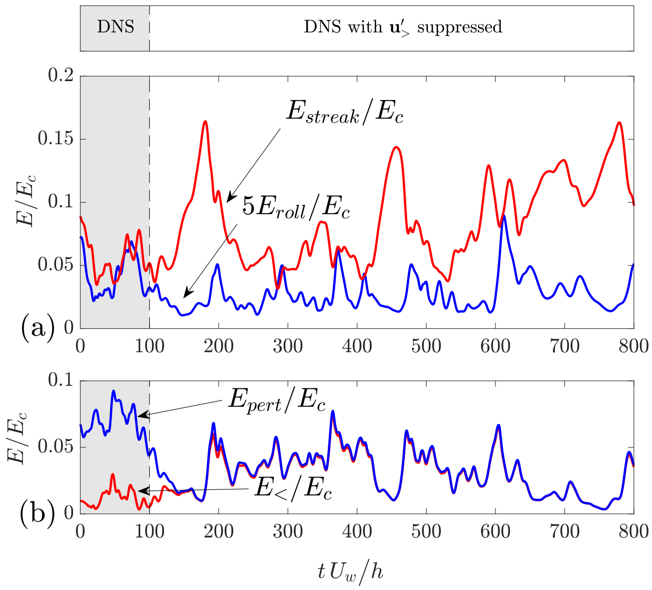

FIGURE 3. (a) Same as Figure 2 but now the complement $\mathbf{u}'_{>}$ is removed with the same protocol. (b) The turbulence sustains in DNS, with the full perturbation field converging to a single LV of the fluctuating mean flow.

cumulant of the perturbation field closed by neglecting the third cumulant. These predictions include identification of the mean and perturbation structures and the physical mechanism supporting the mean flow and the perturbations. The mechanistic component of the SSP that is responsible for supporting the perturbation field and collocating it with the streak so as to maintain the fluctuating streak SSP is identified with the parametric instability of the fluctuating streak. Although the first four LVs of this instability have been verified to account for 20% of the energy of the perturbation field, it is more significant for our purposes that they account for all of the streamwise vorticity forcing that supports the roll component of the roll-streak structure underlying the SSP maintaining the turbulence. Consistently, removal of this small subset of structures is verified to laminarize the turbulence in the DNS.

It is a common assumption that the structure and maintenance of the perturbation field at scales smaller than the integral can be ascribed to a nonlinear cascade and therefore that these scales can be characterized solely by their spectra. We have shown in Couette flow turbulence examined in this work that this is not the case and that these perturbations are maintained primarily by parametric interaction with the mean flow and their structure, rather than being random, can be identified with the LVs associated with this parametric growth process.

These results imply that optimal control strategies based on linearization about the time-dependent streamwise mean flow, which is the first cumulant of the RNL statistical state dynamics, should present substantial advantage over previous optimal control strategies that were based on the instantaneous streamwise and spanwise mean flows (Bewley & Liu 1998; Högberg *et al.* 2003,*a*,*b*; Kim & Bewley 2007). This implication is strengthened by simulations confirming that turbulence is not supported when the fluctuating streaks that are present in the streamwise mean flow are suppressed (Jiménez

& Pinelli 1999). Perhaps most remarkable is the result that a very small subspace of perturbations are responsible for supporting the roll circulation required for maintaining the turbulence. This subspace is much smaller than that maintaining the perturbation variance, demonstrating that suppression of a small subspace of the entire perturbation field is sufficient to laminarize the turbulence.

Acknowledgments

The authors acknowledge use of computational resources from the Certainty cluster awarded by the National Science Foundation to CTR. We would like to thank Prof. Parviz Moin, Prof. Javier Jiménez, Dr. Adrián Lozano-Durán, Dr. Michael Karp, and Dr. Navid Constantinou for their useful comments and discussions. Marios-Andreas Nikolaidis gratefully acknowledges the support of the Hellenic Foundation for Research and Innovation (HFRI) and the General Secretariat for Research and Technology (GSRT). Brian F. Farrell was partially supported by NSF AGS-1640989.

REFERENCES

Adrian, R. J. 2007 Hairpin vortex organization in wall turbulence. *Phys. Fluids* **19**, 041301.

Bakewell Jr., H. P. & Lumley, L. 1967 Viscous sublayer and adjacent wall region in turbulent pipe flow. *Phys. Fluids* **10**, 1880–1889.

Bewley, T. R. & Liu, S. 1998 Optimal and robust control and estimation of linear paths to transition. *J. Fluid Mech.* **365**, 23–57.

Blackwelder, R. F. & Eckelmann, H. 1979 Streamwise vortices associated with the bursting phenomenon. *J. Fluid Mech.* **94**, 577–594.

Bretheim, J. U., Meneveau, C. & Gayme, D. F. 2015 Standard logarithmic mean velocity distribution in a band-limited restricted nonlinear model of turbulent flow in a half-channel. *Phys. Fluids* **27**, 011702.

Budanur, N. B., Short, K. Y., Farazmand, M., Willis, A.P. & Cvitanović, P. 2017 Relative periodic orbits form the backbone of turbulent pipe flow. *J. Fluid Mech.* **883**, 274–301.

Farrell, B. F., Gayme, D. F. & Ioannou, P. J. 2017 A statistical state dynamics approach to wall-turbulence. *Phil. Trans. R. Soc. A* **375**, 20160081.

Farrell, B. F. & Ioannou, P. J. 2003 Structural stability of turbulent jets. *J. Atmos. Sci.* **60**, 2101–2118.

Farrell, B. F. & Ioannou, P. J. 2012 Dynamics of streamwise rolls and streaks in turbulent wall-bounded shear flow. *J. Fluid Mech.* **708**, 149–196.

Farrell, B. F. & Ioannou, P. J. 2017 Statistical state dynamics-based analysis of the physical mechanisms sustaining and regulating turbulence in Couette flow. *Phys. Rev. Fluids* **2**, 084608.

Farrell, B. F., Ioannou, P. J., Jiménez, J., Constantinou, N. C., Lozano-Durán, A. & Nikolaidis, M.-A. 2016 A statistical state dynamics-based study of the structure and mechanism of large-scale motions in plane Poiseuille flow. *J. Fluid Mech.* **809**, 290–315.

Hamilton, K., Kim, J. & Waleffe, F. 1995 Regeneration mechanisms of near-wall turbulence structures. *J. Fluid Mech.* **287**, 317–348.

Herring, J. R. 1963 Investigation of problems in thermal convection. *J. Atmos. Sci.* **20**, 325–338.

Högberg, M., Bewley, T. & Henningson, D. 2003 Relaminarization of Re=100 turbulence using gain scheduling and linear state-feedback control. *Phys. Fluids* **15**, 3572–3575.

Högberg, M., Bewley, T. R. & Henningson, D. S. 2003*a* Linear feedback control and estimation of transition in plane channel flow. *J. Fluid Mech.* **481**, 149–175.

Högberg, M., Bewley, T. R. & Henningson, D. S. 2003*b* Relaminarization of Re=1000 turbulence using linear state-feedback control. *Phys. Fluids* **15**, 3572–3575.

Jiménez, J. 1994 On the structure and control of near wall turbulence. *Phys. Fluids* **6**, 944–953.

Jiménez, J. & Moin, P. 1991 The minimal flow unit in near-wall turbulence. *J. Fluid Mech.* **225**, 213–240.

Jiménez, J. & Pinelli, A. 1999 The autonomous cycle of near-wall turbulence. *J. Fluid Mech.* **389**, 335–359.

Kawahara, G. & Kida, S. 2001 Periodic motion embedded in plane Couette turbulence: regeneration cycle and burst. *J. Fluid Mech.* **449**, 291–300.

Kim, J. & Bewley, T. R. 2007 A linear systems approach to flow control. *Annu. Rev. Fluid Mech.* **39**, 383–417.

Kim, J., Kline, S. J. & Reynolds, W. C. 1971 The production of turbulence near a smooth wall in a turbulent boundary layer. *J. Fluid Mech.* **50**, 133–160.

Kim, J., Moin, P. & Moser, R. 1987 Turbulence statistics in fully developed channel flow at low Reynolds number. *J. Fluid Mech.* **177**, 133–166.

Kline, S. J., Reynolds, W. C., Schraub, F. A. & Runstadler, P. W. 1967 The structure of turbulent boundary layers. *J. Fluid Mech.* **30**, 741–773.

Nikolaidis, M.-A., Farrell, B. F. & Ioannou, P. J. 2018 The mechanism by which nonlinearity sustains turbulence in plane Couette flow. *J. Phys.: Conf. Ser.* **1001**, 012014.

Pausch, M., Yang, Q., Hwang, Y. & Eckhardt, B. 2018 Quasilinear approximation for exact coherent states in parallel shear flows. *Fluid Dyn. Res.* (http://iopscience.iop.org/article/10.1088/1873-7005/aaadcc).

Robinson, S. K. 1991 Coherent motions in the turbulent boundary layer. *Annu. Rev. Fluid Mech.* **23**, 601–639.

Schoppa, W. & Hussain, F. 2000 Coherent structure dynamics in near-wall turbulence. *Fluid Dyn. Res.* **26**, 119–139.

Schoppa, W. & Hussain, F. 2002 Coherent structure generation in near-wall turbulence. *J. Fluid Mech.* **453**, 57–108.

Thomas, V., Farrell, B. F., Ioannou, P. J. & Gayme, D. F. 2015 A minimal model of self-sustaining turbulence. *Phys. Fluids* **27**, 105104.

Thomas, V., Lieu, B. K., Jovanović, M. R., Farrell, B. F., Ioannou, P. J. & Gayme, D. F. 2014 Self-sustaining turbulence in a restricted nonlinear model of plane Couette flow. *Phys. Fluids* **26**, 105112.

Waleffe, F. 1997 On a self-sustaining process in shear flows. *Phys. Fluids* **9**, 883–900.

Waleffe, F. 1998 Three-dimensional coherent states in plane shear flows. *Phys. Rev. Lett.* **81**, 4140–4143.

Waleffe, F. 2001 Exact coherent structures in channel flow. *J. Fluid Mech.* **435**, 93–102.